Wavelength and intensity effects on the dissociation of H_2^+ in intense laser fields

Hongtao Hu,[1,2] Han Xu,[3,*] Ya Bai,[1] R. T. Sang,[3] Igor V. Litvinyuk,[3] Peng Liu,[1,4,†] and Ruxin Li[1,4]

[1]*State Key Laboratory of High Field Laser Physics, Shanghai Institute of Optics and Fine Mechanics, Chinese Academy of Sciences, Shanghai 201800, China*

[2]*University of Chinese Academy of Sciences, Beijing 100049, China*

[3]*Centre for Quantum Dynamics, Griffith University, Nathan, Queensland 4111, Australia*

[4]*Collaborative Innovation Center of IFSA (CICIFSA), Shanghai Jiao Tong University, Shanghai 200240, China*

We report on a systematic investigation of the dissociation dynamics of H_2^+ in intense laser fields, and study how the kinetic energy spectrum of the dissociating proton can be modulated by the wavelength and intensity of the driving laser field. In the experiment, H_2 is dissociatively ionized by an intense laser pulse with varying carrier wavelengths ranging from 800 to 1800 nm and varying peak intensities. A model based on Floquet theory and Landau-Zener theory is adopted to explain the experimental observations. The intensity effect is further explored in a few-cycle pump-probe experiment. We observed a significant intensity-dependent proton kinetic energy shift, which can also be well explained by the theoretical simulation. The wavelength- and intensity-dependent proton spectra reveal the mechanism of selective excitation of vibrational levels of H_2^+ in intense laser fields.

I. INTRODUCTION

The interaction of the simplest molecule, hydrogen, and intense laser fields has been extensively investigated in both experiments [1–4] and theoretical studies [5–7] in order to understand and control the laser-molecule interactions. Photoinduced dissociation and ionization pathways, such as bond softening (BS) [4,8], above-threshold dissociation (ATD) [4,5,9], nonsequential double ionization (NSDI) [2,10], and charge-resonance-enhanced ionization (CREI) [4,11,12], have been discovered. By shaping the temporal profile of the driving laser pulses, such as carrier envelope phase (CEP) controlled few-cycle pulses [13,14], synthesized two-color field [15,16], and pump-probe pulses [17,18], one can not only control the interaction results but also gain deeper understanding of the evolution of electronic and nuclear wave packets [19–21] during the interaction. In addition to the waveform control, the wavelength is also an important parameter for controlling the molecule dissociation and ionization dynamics. In 2003, Niikura *et al.* used a femtosecond laser field with different wavelengths to control the timing of electron-ion recollision in D_2^+ and achieved attosecond resolution for probing the nuclear wave-packet dynamics [22]. In 2008, Litvinyuk *et al.* used a different-wavelengths femtosecond laser field to study the kinetic energy spectrum of D^+ resulting from Coulomb explosion and found that there is a wavelength-dependent high-energy band which is attributed to the three-photon dissociation process [23].

The dissociation dynamics of H_2^+ can be understood by a simple scheme: Upon the first ionization of H_2 a coherent nuclear wave packet (NWP) is promoted to the ground state ($1s\sigma_g$) of H_2^+ and moves outward along the $1s\sigma_g$ potential curve [20]. Efficient coupling between $1s\sigma_g$ and the first repulsive states ($2p\sigma_u$) can be achieved when internuclear separation of H_2^+ reaches to the one-photon or three-photon

avoided crossing [1,20], where H_2^+ dissociates by absorbing or emitting an odd number of photons. The kinetic energy (KE) distribution of protons from dissociation channels is affected by many factors, including the ratio between different dissociation pathways [3,4,24], the internuclear separation of radiative coupling [25,26], the electric field induced Stark shift [1], and the population of vibrational states [3,20,27].

In this paper, we investigate the dissociation dynamics of H_2^+ in infrared intense laser fields. We find that the KE of proton from dissociation of H_2^+ shifts to a lower energy range with increasing carrier wavelength, and the KE distribution is also significantly influenced by the intensity of laser fields. In the few-cycle pump-probe experiment, we further investigate the intensity effect on the dissociation of H_2^+. The measured KE spectrum of protons as a function of time delay shows that the KE shifts to a lower energy range for higher laser intensity. The measurements can be well explained and reproduced by our theoretical simulations. The paper is organized in the following way: Section II introduces the experimental setup and theory model. Section III A discusses the wavelength tuning experiment and wavelength effect. In Sec. III B, we present the few-cycle pump-probe experiment and intensity effect. The summary of this paper is given in Sec. IV.

II. EXPERIMENTAL SETUP AND THEORY MODEL

The three-dimensional momentum distribution of the protons resulting from the dissociation of H_2^+ is measured by using the cold-target recoil ion momentum spectroscopy (COLTRIMS) technique [28], where H_2, introduced by a supersonic jet, is dissociatively ionized by tightly focused laser pulses through a concave mirror ($f = 7.5$ cm). The peak intensity of the laser pulses is calibrated by using the recoil momentum method [29,30]. The acceleration length of the spectrometer in COLTRIMS is 8.1 cm and the drift length is 16.2 cm. With a homogeneous electric field (~ 10 V/cm) applied to the acceleration region which steers the protons toward the detector, a momentum resolution of 0.02–0.05 a.u. can be achieved along the z axis, which is defined as the

———————
*hanxu1981@gmail.com

†peng@siom.ac.cn
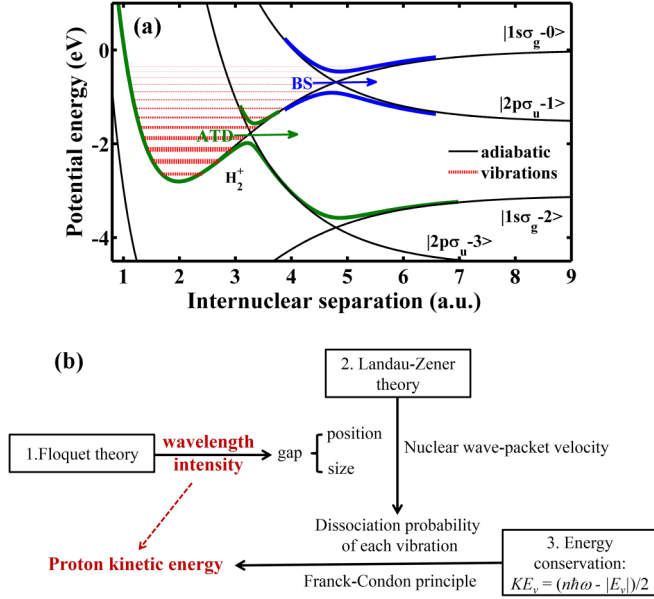
FIG. 1. (a) Schematic picture for the dissociation mechanisms of H_2^+. The black (thin) line labeled "adiabatic" indicates potential curves for the ground state ($1s\sigma_g$) of H_2^+ dressed with $n(n = 0, 2)$ photons and the first excited state ($2p\sigma_u$) of H_2^+ dressed with $m(m = 1, 3)$ photons. The H_2^+ can dissociate through the BS channel [the bold blue (dark gray) line] or the ATD channel [the bold green (light gray) line]. The bold blue (dark gray) line and the bold green (light gray) line are calculated by using Floquet theory [6] at the laser field of 800 nm, 1.0×10^{13} W/cm². The dashed red lines indicate the H_2^+ vibrational levels in the absence of laser fields. The width of the lines indicates the relative population of each vibration state obeying the Frank-Condon distribution [34]. (b) shows the principle of the theory model (for more details please see the text).

direction of flying ions to the microchannel plate (MCP) detector. More details of the experimental setup are given in [31,32].

In the wavelength tuning experiment, the laser pulses with different carrier wavelengths are delivered from a Ti:sapphire laser system (800 nm) and a custom-built three-stage optical parametric amplifier (OPA 1400 and 1800 nm) [31] pumped by the Ti:sapphire laser system. For the few-cycle pump-probe experiment, 6-fs pulses are generated from a neon-filled hollow fiber. This pulse is then split into two pulses via a Mach-Zehnder interferometer, where the intensity of each pulse can be independently controlled by using apertures.

There are mainly three steps [as shown in Fig. 1(b)] to calculate the proton KE from the dissociation of H_2^+ giving the wavelength and intensity of laser fields.

Step 1. The ground-state and excited-state potential of H_2^+ couples in intense laser fields and the energy gap can be calculated using the Floquet theory [1,6,33],

$$E_{\pm}(R) = \frac{V_g(R) + V_u(R) - \hbar\omega}{2}$$
$$\pm \frac{1}{2}\sqrt{[V_g(R) - V_u(R) + \hbar\omega]^2 + (\hbar\omega_R)^2}, \quad (1)$$

where $V_g(R)$ is the potential of the ground state ($1s\sigma_g$) of H_2^+; $V_u(R)$ the potential of the first excited state ($2p\sigma_u$)

of H_2^+; $\hbar\omega$ the photon energy; ω_R the Rabi frequency: $\hbar\omega_R[\text{cm}^{-1}] = E_0 d = 1.17 \times 10^{-3}\sqrt{I[\text{W/cm}^2]}d[\text{a.u.}]$; I the intensity of laser field, d the transition dipole moment; and $E_{\pm}(R)$ the potential curves [6].

Step 2. The dissociation probability of each vibrational state can be calculated from the coupled potentials and the velocity of nuclear motion based on Landau-Zener theory [26,35],

$$P_{L-Z}(v) = 1 - \exp\left(-\frac{\pi}{2\hbar V}\frac{\Delta^2}{|F_1 - F_2|}\right), \quad (2)$$

where $P_{L-Z}(v)$ is the dissociation probability of each vibration state, V the nuclear vibrational motion velocity, Δ the size of the gap, and F the slope of potential curve; Δ and F are calculated from $E_{\pm}(R)$ by Eq. (1).

Step 3. By assuming that the initial vibrational population obeys the Franck-Condon distribution [34], the final proton kinetic energy (E_{PK}) spectrum is given by summing the contributions from all the vibrational states according to the energy conservation formula [3],

$$E_{PK}(E) = \sum_v C_{F-C}(v)P_{L-Z}(v)\exp\left[-\frac{(E_v - E_{Kv})^2}{\Delta E^2}\right], \quad (3)$$

where $C_{F-C}(v)$ is the Frank-Condon distribution of each vibration state, $P_{L-Z}(v)$ the dissociation probability of each vibration calculated in step 2, ΔE the energy width of each vibration, E_{Kv} the proton KE for an individual vibrational level, $E_{Kv} = (n\hbar\omega - |E_v|)/2$, $\hbar\omega$ the photon energy, and E_v the bonding energy of a vibration state v.

We will show that our simulation by this straightforward model generates results consistent with our experimental observations.

III. RESULTS AND DISCUSSIONS

A. Wavelength tuning experiment and wavelength effect

Figure 2 shows the measured KE spectrum of a proton (H^+), which is generated by linearly polarized infrared laser pulses with carrier wavelengths of 800 nm ($\sim$40 fs), 1400 nm ($\sim$50 fs), and 1800 nm ($\sim$50 fs). As we are interested in
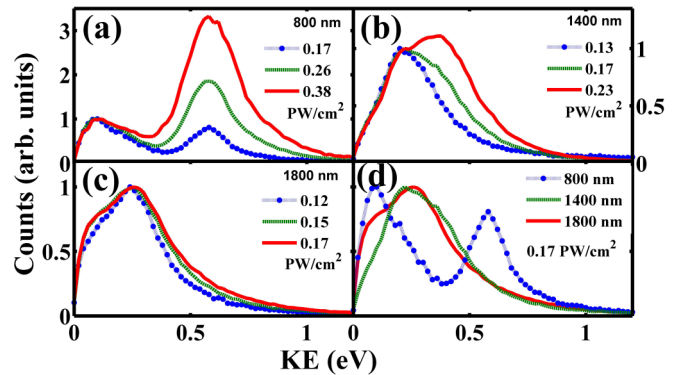
FIG. 2. KE spectrum of proton from dissociation of H_2^+, which is ionized by linearly polarized femtosecond laser pulses with carrier wavelength of (a) 800, (b) 1400, and (c) 1800 nm, respectively. (d) is the KE spectrum measured with 0.17 PW/cm² for all three wavelengths.

the H_2^+ dissociation channel, to preferentially select the H^+ fragments from dissociation channels, we choose those ionization events where only one H^+ is detected. In the experiment, we use a low density of molecules to avoid the space charge effect and the ion signal count rate is as low as 0.05–0.4 per laser shot.

Figure 2(a) shows the measured proton KE spectrum for an 800-nm pulse with three different peak intensities. Comparing with previous results [1,4,25,27], the measured KE spectrum shows a similar double peak structure. The lower-energy peak (at around 0.1 eV) mainly comes from the BS channel which corresponds to one-photon absorption upon dissociation, while the higher-energy peak (at around 0.58 eV) is dominated by the ATD channel, where H_2^+ absorbs three photons at the three-photon avoided crossing followed by emitting one photon at the one-photon avoided crossing. We normalized all the BS peaks for comparison between different laser intensities. ATD yield shows much stronger intensity dependence since it is a multiphoton process and more sensitive to the laser intensity than the BS which is a one-photon process.

Unlike the well separated BS peak and ATD peak for 800 nm, the KE spectrum for 1400 nm does not display a clear double peak structure [see Fig. 2(b)], making it difficult to discriminate the BS and ATD peaks. And more interestingly, the peak position of the KE spectrum for 1400 nm shifts from 0.2 to 0.4 eV when the laser intensity increases from 1.3×10^{14} to 2.3×10^{14} W/cm^2, while in the case of 800 nm the KE spectrum shows a constant peak position for all the intensities scanned. Figure 2(c) shows the KE spectrum for 1800 nm which is similar to that of 1400 nm, but shows a much smaller intensity induced KE peak shift. In Fig. 2(d), the comparison of the KE spectrum for different wavelengths measured with the same intensity (0.17 PW/cm^2) is shown, where we can see the trend that the KE of the proton shifts to as lower energy range with increasing carrier wavelength.

To understand the observed wavelength and intensity dependence, we performed a simulation based on the model introduced in Sec. II, which can assist to resolve the contributions from the BS and ATD processes separately. Figure 3(a) shows the calculated proton kinetic energy spectrum for 800-nm pulses with varying peak intensities. Firstly, the calculated KE of the BS peak (0.1 eV) and ATD peak (0.58 eV) in Fig. 3(a) are in good agreement with the measurements. For the BS process, the one-photon crossing gap opened near the outer turning point of vibrational level 9 ($v = 9$) as shown in Fig. 1. According to the formula $E_k = (n\hbar\omega - |E_{v=9}|)/2$, the kinetic energy contributed by $v = 9$ is 0.4 eV, which is higher than the observed 0.1 eV. However, the barrier near the gap could be suppressed by the laser induced Stark shift, which allows the lower vibrational levels ($v > 5$) to dissociate. Additionally, since the lower vibration levels have a larger population, shown in Fig. 1(a), the contribution to the KE spectrum from $v = 6$ is more dominant than from $v = 9$, which is consistent with the measured BS peak with lower kinetic energy. Secondly, the calculated yield ratio of ATD/BS increases with laser intensity, which agrees qualitatively with the measurements shown in Fig. 2(a). The differences of the ratio of ATD/BS between calculations and measurements may attribute to the focal-volume effect. Figures 3(b) and 3(c) show the calculated KE spectra for 1400 and 1800 nm, respectively. For a 1400-nm
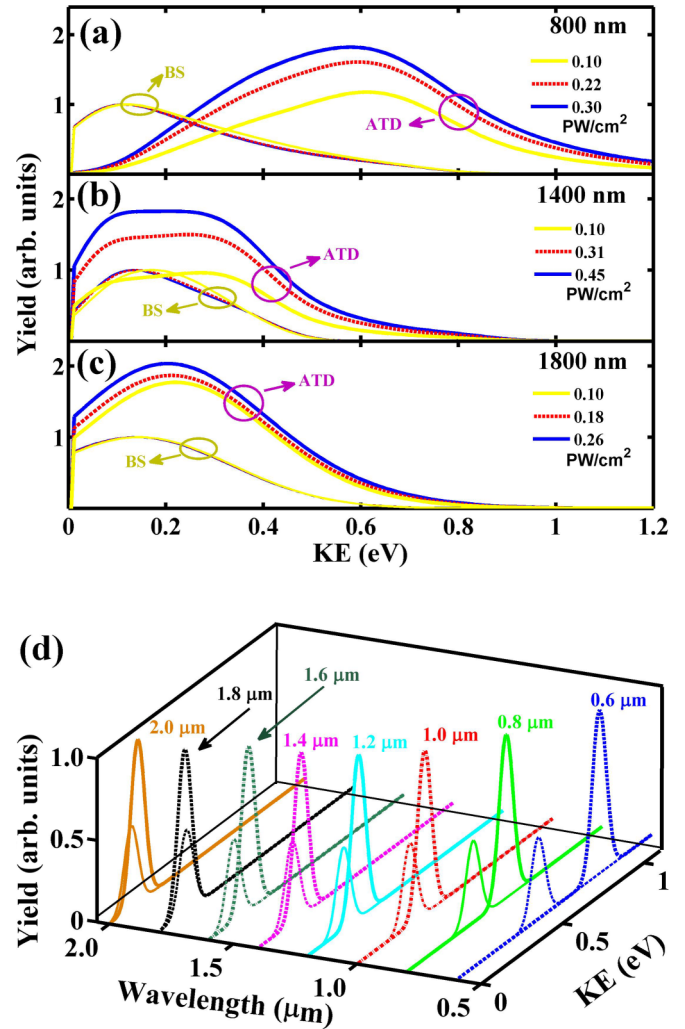
FIG. 3. Calculated proton kinetic energy for (a) 800, (b) 1400, and (c) 1800 nm. As in the measured proton kinetic spectrum, we normalized the BS to unit. (d) shows the kinetic energy spectrum of BS and ATD for different carrier wavelengthsranging from 600 to 2000 nm for the low intensity of 10^{13} W/cm^2 and the pulse duration is 40 fs, where the energy shift due to the intensity effect is ruled out.

pulse, the measured KE spectrum and calculated spectrum both have a very broad single peak structure and the peaks are around 0.2–0.4 eV. Increasing the laser intensity shows that the peak shifts from 0.2 to 0.4 eV. Similarly a single-peak KE spectrum structure and its intensity dependence is also found for 1800-nm pulses. The less resolvable BS peak and ATD peak for longer wavelength can be explained by the low photon energy of the pumping laser, as the energy separation of the two peaks is determined by the photon energy. The calculation shows the peak positions of the BS and ATD channels for both 1400 and 1800 nm are much closer to each other [as shown in Fig. 3(d)] compared to the case of 800-nm pumping. As BS and ATD have different intensity dependence, the yield ratio of ATD/BS changes with the increasing intensity, which is confirmed by the calculation, and also explains the observed changes of the yields of the peaks as shown in Fig. 2(b).

It has been shown that in the electron localization experiments with pumping pulses of 800 nm [13], in order to

observe the interference between the ATD and BS channels, one has to use a few-cycle pulse that has sufficient bandwidth so that the ATD and BS channels can have an overlap in the KE spectrum, as the ATD peak and the BS peak are widely separated. However, our calculation and experiment show that, in the case of infrared pump, the BS peak and ATD peak are almost overlapping even with a multicycle driving pulse, which implies that the electron localization could be achieved even with CEP-stabilized multicycle infrared pulses.

The evolution of the KE spectrum with varying wavelength (from 600 to 2000 nm) is shown in Fig. 3(d); with the increase of the wavelength, the KE spectrum shifts to the lower energy. The coupling (or gap) occurs at those internuclear separations where the energy difference between the ground state and the first repulsive state is equal to the photon energy [6]. For example, the one-photon avoided crossing occurs at the internuclear separation of 4.8 a.u. for the 800-nm intense laser field because the energy difference between the ground state and the first repulsive state is 1.55 eV [20]. And for 1400-nm (1800-nm) intense laser fields, the one-photon gap opens at the distance of 5.5 a.u. (5.9 a.u.). Therefore, for longer carrier wavelengths, the gap opens at a larger internuclear separation which will in turn cause the decrease of the KE of protons [36]. The simulated BS and ATD spectrum shown in Fig. 3(d) is calculated for the low intensity of 10^{13} W/cm^2 and the pulse duration is 40 fs, where the energy shift due to the intensity effect is ruled out [26].

B. Few-cycle pump-probe experiment and intensity effect

According to the Floquet theory [6], the increased laser intensity can suppress the barrier potential of the coupling states even more [7], so that the lower-vibrational-level molecules are able to be excited to generate the low-energy protons [36]. In the single-pulse wavelength tuning experiment, H_2^+ is generated at the peak of the pulse while the dissociation process happens at its tail. When we modulate the intensity around the tail of the pulse, we also modulate its peak intensity, which can lead to a high double ionization probability and consequently the depletion of H_2^+. To avoid the depletion, the intensity scan has to be limited to a small range, making it hard to observe an obvious intensity-dependent KE shift. In order to confirm this intensity effect experimentally, we propose a few-cycle pump-probe experiment. The full width at half maximum (FWHM) of the few-cycle pulse is 6 fs, and the intensities of the pump pulse and the probe pulse are 6.0×10^{14} and 6.0×10^{13} W/cm^2, respectively. The polarizations of pump pulse and probe pulse are both linear and parallel to each other. The time delay between the pump and probe pulses is scanned from 5 to 45 fs with a step of 0.67 fs.

As shown in Fig. 4(a), the neutral H_2 is singly ionized by the pump pulse, which initiates the NWP propagation along the potential curve of the $1s\sigma_g$ state. The probe pulse is then applied while the NWP is passing the one-photon avoided crossing ($R = 4.8$ a.u. for 800 nm). By tuning the time delay between pump and probe pulses, we can modulate the instantaneous intensity at the moment when the one-photon excitation happens, which can in turn modulate the KE of the BS peak. As the probe pulse is extremely short ($\sim$6 fs), which is comparable with the time for the NWP reaching the
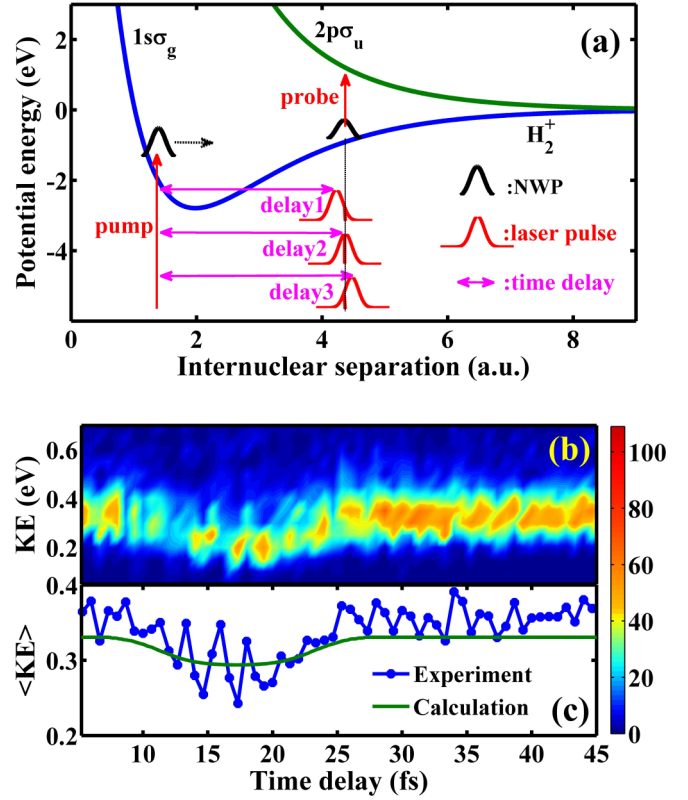
FIG. 4. (a) The NWP will experience different intensity with different time delay at the coupling point, which can lead to different laser induced Stark shift. For example, the Stark shift effect is more distinct at delay2 than at delay1 or delay3. (b) The measured KE spectrum of the dissociation channel as a function of time delay. (c) The comparison of measured averaged KE and calculated averaged KE. The averaged KE minimizes at the time delay of $\sim$15 fs.

one-photon avoided crossing, it is possible to observe a clear delay-dependent KE modulation of the BS peak.

Figure 4(b) shows the measured KE (KE is half of the kinetic energy release of dissociation of H_2^+ [3,20,26]) spectrum as a function of time delay. To highlight the dissociation channel, we only show the spectrum of a proton with KE less than 0.7 eV. The higher-energy double ionization channels, especially the CREI channel with a double peak structured R-dependent ionization rate, can be found in [37]. As expected, the measured KE spectrum shows a distinct delay dependence. The KE shifts to lower energy around a delay time of 15 fs, which indicates that it took $\sim$15 fs for the initial NWP to reach the one-photon avoided crossing. For other delays, the BS energy shows a much weaker delay dependence, because the Stark shift is mainly produced by the tail of the pump pulse. To evaluate the shift of KE quantitatively for better comparison with the simulation, we plot the weighted averaged KE using

$$\langle E \rangle = \frac{\sum_{E=0\,\text{eV}}^{0.7\,\text{eV}} E C(E)}{\sum_{E=0\,\text{eV}}^{0.7\,\text{eV}} C(E)}, \qquad (4)$$

where $\langle E \rangle$ is the weighted averaged KE and $C(E)$ is the counts at the KE of E.

In the simulation, we use a 6-fs Gaussian pulse with carrier wavelength of 800 nm and peak intensity of 10^{14} W/cm^2, and

the laser intensity that causes the dissociation of H_2^+ is given by $I(\tau) = I_0 \exp[-(\tau - t_0)^2/\tau_0^2]$, where $\tau_0 = 6$ fs is the pulse duration; t_0 is set as 15 fs to match the measured delay time for NWP to reach one-photon avoided crossing.

The measured delay-dependent averaged KE and the corresponding calculation are shown in Fig. 4(c). Both show a similar delay-dependent shift (0.1–0.2 eV), which can be explained by the delay-dependent Stark shift. We note that the measured KE spectrum in Fig. 4(b) oscillates at the laser oscillation period (2.7 fs). The oscillations come from the intensity modulation due to the interference between the probe pulse and the tail of the pump pulse. At the constructive interference time delay, the proton yields increase for the high intensity and vice versa. So we can see the periodic modulation of the yield in the measured kinetic energy spectrum as a function of time delay. In the simulation, we ignore the interference effect and only consider the probe laser fields, so there are no oscillations in the simulation shown in Fig 4(c). The measured delay-dependent averaged KE spectrum which shows a maximum modulation amplitude around 15 fs indicates that it takes the initial Frank-Condon NWP about 15 fs to reach the one-photon avoided crossing.

IV. SUMMARY

We experimentally investigate how the wavelength and intensity of the driving laser field can affect the kinetic energy of the proton from dissociation of H_2^+. To study the wavelength effect, H_2^+ is dissociatively ionized using a single pulse with varying carrier wavelengths; we find that the KE spectrum shifts to lower kinetic energy with increasing wavelength under the same intensity and the yield ratio of ATD and/or BS increases with the increasing of laser intensity. In the few-cycle pump-probe experiment we explore the intensity effect, where the intensity of one-photon excitation taking place is modulated by changing the delay between pump and probe, which in turn modulates the strength of the laser induced Stark shift. We find that the higher laser intensity can shift the BS peak to lower kinetic energy. A model based on Floquet theory and Landau-Zener theory can reproduce the experimental observations very well. The wavelength- and intensity-dependent proton spectra reveal the mechanism of selective excitation of vibrational levels of H_2^+ in intense laser fields.

[1] J. H. Posthumus, Rep. Prog. Phys. **67**, 623 (2004).

[2] H. Niikura, F. Legare, R. Hasbani, A. D. Bandrauk, M. Y. Ivanov, D. M. Villeneuve, and P. B. Corkum, Nature **417**, 917 (2002).

[3] T. D. G. Walsh, F. A. Ilkov, and S. L. Chin, J. Phys. B **30**, 2167 (1997).

[4] G. N. Gibson, M. Li, C. Guo, and J. Neira, Phys. Rev. Lett. **79**, 2022 (1997).

[5] G. Jolicard and O. Atabek, Phys. Rev. A **46**, 5845 (1992).

[6] E. E. Aubanel, J. M. Gauthier, and A. D. Bandrauk, Phys. Rev. A **48**, 2145 (1993).

[7] A. Giustisuzor, F. H. Mies, L. F. Dimauro, E. Charron, and B. Yang, J. Phys. B **28**, 309 (1995).

[8] P. H. Bucksbaum, A. Zavriyev, H. G. Muller, and D. W. Schumacher, Phys. Rev. Lett. **64**, 1883 (1990).

[9] A. Giusti-Suzor, X. He, O. Atabek, and F. H. Mies, Phys. Rev. Lett. **64**, 515 (1990).

[10] A. S. Alnaser, X. M. Tong, T. Osipov, S. Voss, C. M. Maharjan, P. Ranitovic, B. Ulrich, B. Shan, Z. Chang, C. D. Lin, and C. L. Cocke, Phys. Rev. Lett. **93**, 183202 (2004).

[11] T. Zuo and A. D. Bandrauk, Phys. Rev. A **52**, R2511 (1995).

[12] E. Constant, H. Stapelfeldt, and P. B. Corkum, Phys. Rev. Lett. **76**, 4140 (1996).

[13] M. F. Kling, C. Siedschlag, A. J. Verhoef, J. I. Khan, M. Schultze, T. Uphues, Y. Ni, M. Uiberacker, M. Drescher, F. Krausz, and M. J. Vrakking, Science **312**, 246 (2006).

[14] N. G. Kling, K. J. Betsch, M. Zohrabi, S. Zeng, F. Anis, U. Ablikim, B. Jochim, Z. Wang, M. Kubel, M. F. Kling,

K. D. Carnes, B. D. Esry, and I. Ben-Itzhak, Phys. Rev. Lett. **111**, 163004 (2013).

[15] B. Sheehy, B. Walker, and L. F. DiMauro, Phys. Rev. Lett. **74**, 4799 (1995).

[16] V. Wanie, H. Ibrahim, S. Beaulieu, N. Thiré, B. E. Schmidt, Y. Deng, A. S. Alnaser, I. V. Litvinyuk, X.-M. Tong, and F. Légaré, J. Phys. B **49**, 025601 (2016).

[17] T. Ergler, A. Rudenko, B. Feuerstein, K. Zrost, C. D. Schroter, R. Moshammer, and J. Ullrich, Phys. Rev. Lett. **95**, 093001 (2005).

[18] X. C. Gong, P. L. He, Q. Y. Song, Q. Y. Ji, H. F. Pan, J. X. Ding, F. He, H. P. Zeng, and J. Wu, Phys. Rev. Lett. **113**, 203001 (2014).

[19] U. Thumm, T. Niederhausen, and B. Feuerstein, Phys. Rev. A **77**, 063401 (2008).

[20] C. R. Calvert, W. A. Bryan, W. R. Newell, and I. D. Williams, Phys. Rep. **491**, 1 (2010).

[21] Y. Nabekawa, Y. Furukawa, T. Okino, A. Amani Eilanlou, E. J. Takahashi, K. Yamanouchi, and K. Midorikawa, Nat. Commun. **6**, 9197 (2015).

[22] H. Niikura, F. Legare, R. Hasbani, M. Y. Ivanov, D. M. Villeneuve, and P. B. Corkum, Nature **421**, 826 (2003).

[23] I. V. Litvinyuk, A. S. Alnaser, D. Comtois, D. Ray, A. T. Hasan, J. C. Kieffer, and D. M. Villeneuve, New J. Phys. **10**, 083011 (2008).

[24] D. S. Murphy, J. McKenna, C. R. Calvert, W. A. Bryan, E. M. L. English, J. Wood, I. C. E. Turcu, W. R. Newell, I. D. Williams, and J. F. McCann, J. Phys. B **40**, S359 (2007).

[25] M. R. Thompson, M. K. Thomas, P. F. Taday, J. H. Posthumus, A. J. Langley, L. J. Frasinski, and K. Codling, J. Phys. B **30**, 5755 (1997).

[26] A. Zavriyev, P. H. Bucksbaum, H. G. Muller, and D. W. Schumacher, Phys. Rev. A **42**, 5500 (1990).

[27] I. D. Williams, P. McKenna, B. Srigengan, I. M. G. Johnston, W. A. Bryan, J. H. Sanderson, A. El-Zein, T. R. J. Goodworth, W. R. Newell, P. F. Taday, and A. J. Langley, J. Phys. B **33**, 2743 (2000).

[28] J. Ullrich, R. Moshammer, A. Dorn, R. Dorner, L. P. H. Schmidt, and H. Schmidt-Bocking, Rep. Prog. Phys. **66**, 1463 (2003).

[29] A. S. Alnaser, X. M. Tong, T. Osipov, S. Voss, C. M. Maharjan, B. Shan, Z. Chang, and C. L. Cocke, Phys. Rev. A **70**, 023413 (2004).

[30] C. Smeenk, J. Z. Salvail, L. Arissian, P. B. Corkum, C. T. Hebeisen, and A. Staudte, Opt. Express **19**, 9336 (2011).

[31] C. Li, D. Wang, L. W. Song, J. Liu, P. Liu, C. H. Xu, Y. X. Leng, R. X. Li, and Z. Z. Xu, Opt. Express **19**, 6783 (2011).

[32] P. Peng, S. C. Peng, H. T. Hu, N. Li, Y. Bai, P. Liu, H. L. Xu, R. X. Li, and Z. Z. Xu, Opt. Express **23**, 18763 (2015).

[33] X. He, O. Atabek, and A. Giusti-Suzor, Phys. Rev. A **38**, 5586 (1988).

[34] G. H. Dunn, J. Chem. Phys. **44**, 2592 (1966).

[35] C. Zener, Proc. R. Soc. London, Ser. A **137**, 696 (1932).

[36] T. D. G. Walsh, F. A. Ilkov, S. L. Chin, F. Chateauneuf, T. T. Nguyen-Dang, S. Chelkowski, A. D. Bandrauk, and O. Atabek, Phys. Rev. A **58**, 3922 (1998).

[37] H. Xu, F. He, D. Kielpinski, R. T. Sang, and I. V. Litvinyuk, Sci. Rep. **5**, 13527 (2015).